ELSEVIER

Journal of Nuclear Materials 290–293 (2001) 812–819

journal of nuclear materials

www.elsevier.nl/locate/jnucmat

The effect of baffling on divertor leakage in Alcator C-Mod

C.S. Pitcher [a,*], C.J. Boswell [a], T. Chung [a], J.A. Goetz [a], B. LaBombard [a], B. Lipschultz [a], J.E. Rice [a], D.P. Stotler [b], J.L. Terry [a]

[a] *Plasma Science and Fusion Center, MIT, NW17-111, 175 Albany Street, Cambridge, MA 02139-4307, USA*
[b] *Princeton Plasma Physics Lab, Princeton, NJ 08543, USA*

Abstract

The effect of divertor baffling on Alcator C-Mod has been investigated using a novel divertor bypass. The bypass allows in situ variations in the leakage conductance between the divertor plenum and the main chamber. The experimental results, supported by simple modeling, suggest that C-Mod operates in a regime where the leakage flux is independent of the leakage conductance. The relatively large leakage flux is driven by the high gas pressure in the C-Mod divertor and is 'flux-limited' by the atom creation rate at the target plate and the atom escape probability from the divertor plasma. These results, along with results from other tokamaks, suggest that baffling needs to be significantly tighter than had been previously thought to ensure low levels of divertor leakage and maximum divertor pressures. © 2001 Elsevier Science B.V. All rights reserved.

Keywords: Alcator C-Mod; 1D model; Divertor pumping

1. Introduction

It has long been thought in tokamak research that tight divertor baffling improves discharge performance. This has primarily been attributed to reducing the level of hydrogenic neutrals in the main chamber. This was the conclusion from early research on PDX [1] and ASDEX [2], which showed improved levels of global energy confinement with increased levels of divertor closedness. More recently, however, experiments on JET [3–5], ASDEX-Upgrade [6–8], DIII-D [9] and JT-60U [10] have not shown improvements in confinement as the baffle structures have become more closed, although certainly changes in the divertor behavior were observed.

In addition to the possible effect on confinement, there are potentially other beneficial effects associated with increasing divertor closedness, e.g. an increase in the hydrogenic and helium 'ash' gas pressures in the divertor, which in the presence of pumping, makes it easier to control plasma density and core helium content. In the case of gaseous impurities, both intrinsic and intentionally added (e.g., neon, argon, etc.), tighter baffling may result in better screening of these impurities from the plasma core.

One problem with research on divertor baffling is that geometry comparisons are typically made across different experimental campaigns, with varying magnetic geometries, machine conditions and diagnostic arrangements. Results and conclusions, therefore, are sometimes uncertain. We have attempted to address this problem in previous research by constructing a novel divertor baffle that can be altered in situ, between discharges and even during discharges. The effect of variations in divertor baffling are therefore made under identical operating conditions, eliminating much of the uncertainty present in previous experimental results. We call this hardware the Alcator C-Mod divertor bypass.

2. Experiment

Alcator C-Mod is a relatively small, high-field tokamak, with a single-null (bottom) divertor, ICRF heating

* Corresponding author.
E-mail address: csp@psfc.mit.edu (C.S. Pitcher).

0022-3115/01/$ - see front matter © 2001 Elsevier Science B.V. All rights reserved.
PII: S0022-3115(00)00537-7

and molybdenum first-walls which are routinely boronized [11]. A poloidal cross-section of the machine appears in Fig. 1. Under normal operating conditions, gas leakage from the divertor to the main chamber is either through the divertor plasma fan and X-point regions via charge-exchange diffusion of atoms (which we believe is relatively small due to the opacity of the plasma in this region, except at low discharge density [12]), or occurs through gaps behind the mechanical structure that supports the outer divertor plate. The exact magnitude of this latter, intrinsic leakage 'conductance' is not known precisely, but is estimated to be $\approx 20\ m^3\ s^{-1}$ (free-molecular). The region behind the outer target plate, the plenum, is fed with neutrals from the private flux region through a gap at the bottom of the outer target plate. The conductance of this gap is relatively large, $>40\ m^3\ s^{-1}$, and plays only a minor role in determining the flux through the leakage path.

The conductance between the divertor plenum and the main chamber is altered in these experiments using the Alcator C-Mod divertor bypass, Fig. 1 [13] which has a free-molecular conductance of $\sim 23\ m^3\ s^{-1}$. This is comparable to the intrinsic leakage conductance and thus, the opening of the bypass effectively doubles the leakage conductance.

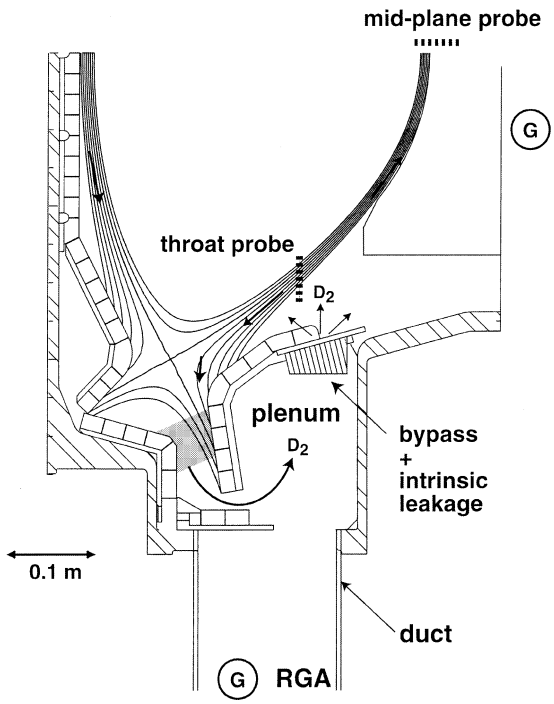

Fig. 1. Poloidal cross-section of the lower half of Alcator C-Mod showing the location of the divertor bypass and various edge/divertor diagnostics. 'G' denotes pressure gauge, 'RGA' denotes residual gas analyzer. The circulation of gas through the bypass and returning to the divertor as ion flow in the SOL is illustrated. The shaded region in the divertor represents the region modeled in Section 4.

C-Mod has a large number of edge and divertor diagnostics (see Fig. 1), including fixed Langmuir probes incorporated into the inner and outer divertor plates (not shown), fast-scanning Langmuir/Mach probes (outer divertor throat and mid-plane), an absolute MKS pressure gauge and residual gas analyzer (RGA) at the end of a long tube ($\sim$1.7 m) connected to the divertor, and an ionization gauge at the outside mid-plane [14].

3. Experimental results

We have performed experiments investigating the effect of the bypass on the divertor and main plasma conditions, focusing in this paper on the effect on the hydrogenic behavior, including the effect on gas pressures, recycling fluxes and divertor plasma conditions. The effects on energy confinement and impurity screening are covered in other papers [15,16].

3.1. Effect on gas pressures

We have made comparisons between discharges with the bypass open versus similar discharges with the bypass closed. Fig. 2 gives the mid-plane and divertor D_2 pressures as functions of the line-averaged density from an Ohmic density scan (990 429, two data points per discharge). All gas pressures in C-Mod, regardless of poloidal location, increase with discharge density, and this is clearly shown. In the case of the mid-plane pressure, the effect is strongly non-linear, i.e., $\propto \bar{n}_e^4$. One notes, however, that within the scatter of the data, there

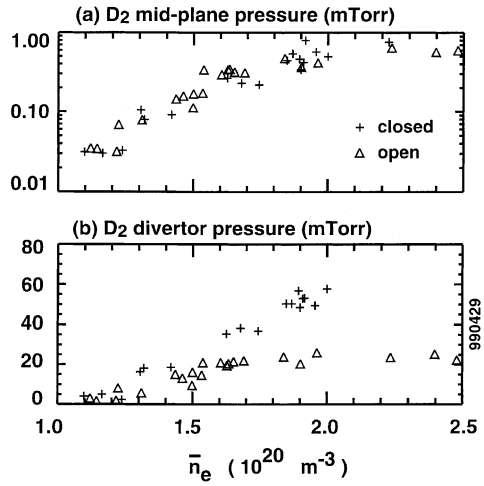

Fig. 2. The deuterium (a) mid-plane pressure (b) divertor pressure as functions of discharge density for the Ohmic density scan. Comparison between bypass open and closed.

is no apparent effect of the bypass on the mid-plane pressure. This contrasts with the divertor pressure, Fig. 2(b), which clearly shows the effect of the bypass at moderate and high plasma density, typically showing a factor ~2 decrease in pressure at the same discharge density with the bypass open. This factor of ~2 is common to all C-Mod discharges at moderate and high density, including Ohmic, L-mode and H-mode discharges. The effect is weaker at low plasma density.

The fact that the divertor pressure drops by factor of ~2 when the conductance between the divertor plenum and mid-plane increases by a factor of ~2, suggests that the gas leakage flux is constant, independent of the conductance. Thus, the insensitivity of the mid-plane pressure to the bypass appears therefore to be due, at least in part, to a leakage flux which is approximately constant. The dependence on the bypass would be further weakened by recycling of plasma off of limiters and antennas in the main chamber, which also generates significant quantities of gas [12,17]. A possible causal relationship between the two sources of main chamber gas is still under investigation.

3.2. Effect on recycling fluxes

At first sight one would expect that a significant change in the conductance between the divertor plenum and the main chamber, resulting in a factor ~2 change in divertor pressure, should result in changes in the divertor and main chamber conditions. Surprisingly, very little effect is observed. Fig. 3 gives the recycling fluxes from the Ohmic density scan at (a) the outer plate, derived from the built-in Langmuir probes and spatially integrated, (b) the leakage flux through the outer divertor plate structure, based on the estimated conductance and the divertor gas pressure and (c) the plasma flow towards the divertor as deduced by the 'throat' Mach probe [12]. Data points are distinguished by whether the bypass is open or not.

In the case of the outer plate flux, Fig. 3(a), the rapid increase with plasma density is characteristic of high recycling divertor operation, with the 'roll-over' and decrease at high density indicating plasma detachment [18]. The bypass has no effect on this recycling, despite the factor of ~2 change in divertor D_2 pressure just outside of the divertor plasma.

As implied in the last section, Fig. 3(b) demonstrates that the leakage flux, although increasing rapidly with plasma density, shows no dependence on the bypass, i.e. on the leakage conductance.

The plasma flux to the outer divertor through the outer throat based on the throat Mach probe, Fig. 3(c), is consistent with the other measurements, also indicating no effect due to the bypass. While the absolute determination of the throat flux is uncertain since it relies on an uncertain theoretical model [12,19], the measurement should be sensitive to the flow induced as gas released by the bypass into the main chamber is ionized and returns to the divertor as plasma flow in the SOL. The probe's sensitivity to this induced flow would be weakened by the fact that only a fraction of the leakage flux is expected to be ionized above the position of the probe. Nevertheless, some difference might be expected as a result of a change in leakage flux, but none is observed.

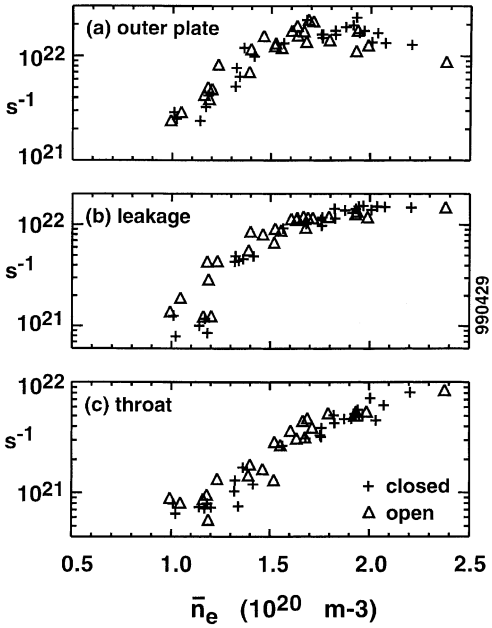

Fig. 3. Recycling fluxes in the Ohmic density scan: (a) the spatially-integrated ion flux to the outer plate based on built-in Langmuir probes; (b) the atom leakage flux through the outer divertor structure based on the calculated conductance and the divertor plenum pressure; (c) radially-integrated SOL plasma flow through the 'throat' towards the outer divertor. Comparison between bypass open and closed.

The leakage flux is large in relative terms. Fig. 4 gives the leakage flux normalized by the integrated ion flux to the outer plate. In the range of ~50% of ions striking the outer plate recycle to the plasma, not in the divertor, but to the main chamber through the leakage conductance. This determination, using only the Langmuir probes for the atom creation rate, does not take into account volume recombination. This is believed to be small in the outer plasma fan at low and moderate density, but becomes comparable to the ion plate source under strongly detached conditions, i.e., $\bar{n}_e > 2 \times 10^{20}$ m^{-3}. This could be the explanation for the leakage to plate flux ratio rising above 1 above this plasma density, bearing in mind that the estimated error associated with this ratio is approximately a factor ~2. Nevertheless, a large fraction of atoms generated at the outer divertor plate re-enter the plasma outside of the divertor.

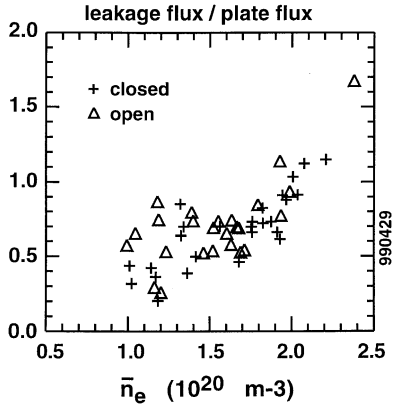

Fig. 4. The ratio of leakage flux to outer plate flux (from Fig. 3). Comparison between bypass open and closed.

3.3. Effect on divertor plasma conditions

The recycling ion flux at the outer plate in Fig. 3(a) shows little effect of the bypass. More details on the plasma conditions at the outer plate are given in Fig. 5, where the plasma density n_t and temperature T_t at the outer divertor target plate deduced by the build-in Langmuir probes are given for a flux surface ~1 mm from the strike-point (mid-plane equivalent). As has been well-established in a variety of divertor tokamaks [20], the rapid increase of n_t with plasma density is indicative of high recycling conditions, and the eventual 'roll-over' at temperatures $T_t < 5$ eV evidence for plasma detachment [18]. As above, the bypass has no effect on this behavior, despite the usual factor ~2 difference in divertor gas pressure outside the plasma fan. These results are again surprising, particularly in the case of the detachment behavior, since the plasma pressure loss along field lines which gives rise to the drop in the plasma density adjacent to the plate is thought to be due to the friction of ions on neutral atoms and molecules as they travel towards the target plate [18]. Evidently, the ion-neutral friction inside the plasma is not influenced by the gas pressure immediately outside the plasma. In the next section we will show from the modeling that, indeed, the neutral atom density inside the plasma fan is relatively insensitive to changes in the neutral molecular density outside the fan. This is consistent with experimental divertor D_α measurements at the outer plate (not shown), which show no effect of the bypass. The D_α measurement, under attached conditions (low volume recombination), is a direct measure of the recycling flux at the outer plate.

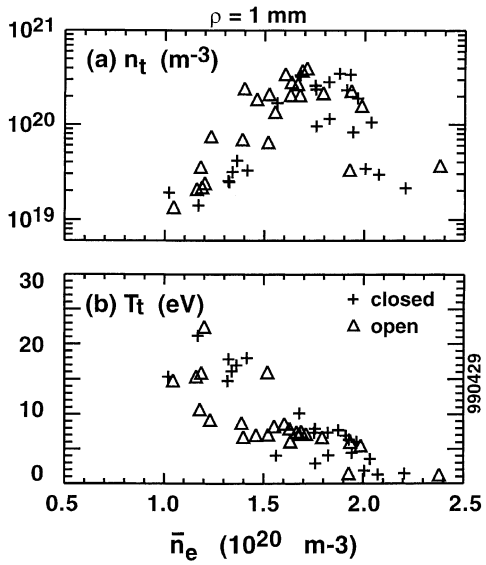

Fig. 5. Divertor target plate plasma density n_t and electron temperature T_t for the Ohmic density scan. Comparison between bypass open and closed.

4. Analytic model

In this section we gain insight into these experimental results using a simple 1D analytic model. We adopt a philosophy of developing the simplest physical model which can reproduce the basic experimental results. The model is not meant to be numerically correct in an absolute sense, but rather to identify the key processes and trends.

We consider the shaded region in the outer divertor indicated in Fig. 1, which straddles the separatrix, extending from the target plate to the wall in the private flux region. Fig. 6 gives a schematic representation of this region. Region I consists of the divertor plasma, which is considered stationary in the relevant direction 'x' across field lines. The width of Region I, identified with the density width at the plate λ_{plate}, varies in C-Mod depending on the global plasma conditions. For high recycling conditions, the focus of our modeling

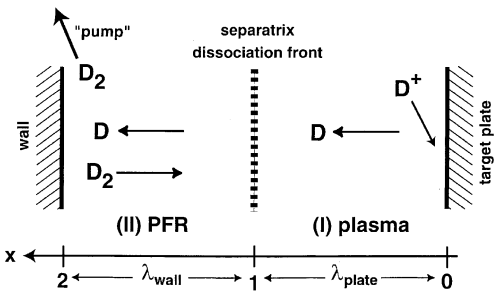

Fig. 6. Schematic figure used in the simple modeling, representative of the shaded region in Fig. 1.

presented here, typically $\lambda_{\text{plate}} \sim 1$ cm. Deuterons incident on the plate are assumed to be promptly converted to atoms (molecular effects are neglected here), which then move toward the private flux region (PFR, Region II). In their transit across the plasma, the atoms experience ionization and charge-exchange/elastic scattering. If they escape the plasma they continue to travel into the PFR until they eventually reach the wall, where they are converted to molecules. At the wall, a fraction (the 'pump fraction' f) of the mean random thermal flux of molecules is 'pumped' through the bypass and/or other leaks in the divertor structure. The pump fraction is estimated from details of the divertor three-dimensional geometry to be $f \approx 0.15$ with the bypass closed, and double this with the bypass open, i.e., $f \approx 0.30$. Those molecules not pumped, travel back towards the plasma and it is assumed that they are dissociated to atoms promptly on reaching the separatrix at a 'dissociation front', thus adding particles (but not momentum) to the atom flux out of the plasma. The recycling molecules flow against the outflux of relatively energetic atoms and, depending on their density, can exchange momentum. This latter effect tends to increase the molecular pressure, while having little affect on the atoms (which tend to be at much higher pressure). We assume a constant temperature T for the atoms in the two regions, equal to the plasma temperature $T = T_t$ (we assume equal ion and electron temperatures in the divertor plasma $T_e = T_i = T_t$), and a significant lower molecular temperature, T_m, close to the wall surface temperature. In C-Mod, the width of Region II (i.e. the typical separatrix to wall separation) is $\lambda_{\text{wall}} \sim 10$ cm.

4.1. Balance equations in Region I

We write the following particle and momentum balance equations for the atoms in Region I

$$\frac{\mathrm{d}(nv)}{\mathrm{d}x} = -S_i, \tag{1}$$

$$\frac{\mathrm{d}(nT + mnv^2)}{\mathrm{d}x} = -mvS_m - mvS_i, \tag{2}$$

where n, v, m are the atom density, velocity and mass. S_i and S_m are the ionization and momentum loss rates (charge-exchange + elastic scattering) for the atoms as they interact with the plasma ions and electrons as they traverse Region I

$$S_i = nn_t\langle\sigma v\rangle_i, \tag{3}$$

$$S_m = nn_t\langle\sigma v\rangle_m, \tag{4}$$

where $\langle\sigma v\rangle_i$ and $\langle\sigma v\rangle_m$ are the corresponding rate coefficients, assumed for simplicity to be only functions of the common atom and plasma temperature T. The plasma conditions, n_t and T_t are assumed constant in space.

These equations can be solved analytically, yielding the following:

$$\frac{n_1}{n_0} = \left[\frac{M^{*2} - M_1^2}{M^{*2} - M_0^2}\right]^{(2\alpha-1)/2(1-\alpha)}, \tag{5}$$

$$g(M_0) - g(M_1) = \frac{\lambda_{\text{plate}}}{\lambda_i}, \tag{6}$$

where '0' denotes the conditions at the target plate and '1' at the separatrix. We define the atom Mach number $M \equiv v/c$, where $c = (T/m)^{1/2}$ is the atom sound speed and where we further define

$$\begin{aligned} g(M) &\equiv M - \frac{2\alpha - 1}{2\alpha^{1/2}(1-\alpha)^{1/2}} \ln\left[\frac{M^* + M}{M^* - M}\right], \\ M^* &\equiv \left(\frac{\alpha}{1-\alpha}\right)^{1/2}, \quad \alpha \equiv \frac{\langle\sigma v\rangle_i}{\langle\sigma v\rangle_i + \langle\sigma v\rangle_m}, \\ \lambda_i &\equiv \frac{cM^{*2}}{n_t\langle\sigma v\rangle_i}. \end{aligned} \tag{7}$$

4.2. Balance equations in Region II

In Region II, there are no volume sources/sinks for particles, although we must now consider the momentum balance for both atoms and molecules and their coupling

$$\frac{\mathrm{d}(nT + mnv^2)}{\mathrm{d}x} = -m(v - v_m)S_{am}, \tag{8}$$

$$\frac{\mathrm{d}\left(n_mT_m + 2mn_mv_m^2\right)}{\mathrm{d}x} = -m(v_m - v)S_{am}, \tag{9}$$

where n_m, v_m are the molecular density and flow velocity and S_{am} is the rate coefficient for momentum transfer collisions between atoms and molecules

$$S_{am} = nn_m\langle\sigma v\rangle_{am}. \tag{10}$$

We proceed by neglecting the molecular velocity v_m compared with v in Eqs. (8) and (9). Thus, the right-hand sides of these equations become $\mp mvS_{am}$, respectively. This simplification allows the entire set of equations, Eqs. (1)–(10), to be solved without finite difference techniques, but still numerically.

4.3. Boundary conditions

The following boundary conditions apply to the problem. At the right boundary '0' (the target plate), the atom flux density $\phi_0 = n_tc_{st}\sin\theta$ is determined by the divertor plasma and magnetic geometry (θ is the angle of the field line with the plate, $\sin\theta \approx 0.01$ and c_{st}

is the ion acoustic speed, $c_{st} = (2T_t/m)^{1/2}$). We assume that n_t, T_t are fixed and determined by the upstream conditions, i.e., by the mid-plane plasma density and power entering the SOL. (This assumption is a result of the standard two-point SOL model, and is only approximately correct in the face of varying levels of parallel field heat convection [21].)

At the interface '1', atom flux density and total atom pressure (static + dynamic) are conserved, the molecules coming from the wall are assumed to meet the plasma at their sound speed, i.e., flowing at $v_m = -c_m$, where $c_m = (T_m/2m)^{1/2}$. At the left boundary '2', a fraction f of the molecular mean random flux is 'pumped' (the pump fraction mentioned earlier) and this is equal to the atom flux which escapes the plasma without being ionized ϕ_1, i.e. $\phi_1 = \frac{1}{2} n_{m2} \bar{c}_m f$, where $\bar{c}_m$ is the molecular thermal speed. The atoms at '2' are assumed to be flowing to the wall with their sound speed.

4.4. Model results

Fig. 7 gives results from the model for the Mach number, density, flux density and total pressure for atoms and molecules for a case corresponding to C-Mod at moderate plasma density, $\bar{n}_e \approx 1.5 \times 10^{20}$ m^{-3} (high recycling conditions). We assume divertor plasma conditions close to that measured with the plate probes, $\lambda_{plate} = 0.5$ cm, $n_t = 1.8 \times 10^{20}$ m^{-3}, $T_t = 5$ eV and rate coefficients $\langle \sigma v \rangle_i = 2.6 \times 10^{-15}$ m^3 s^{-1}, $\langle \sigma v \rangle_m = 1.8 \times 10^{-14}$ m^3 s^{-1}, $\langle \sigma v \rangle_{am} = 2.0 \times 10^{-15}$ m^3 s^{-1}. The molecules are assumed to be cold in relation to the atoms, i.e. $T_m = 0.1$ eV. The hardware geometry is taken account using $\lambda_{wall} = 10$ cm and $f = 0.15$ (bypass closed). The horizontal axis is the spatial dimension, but one notes the different scale-lengths in Regions I and II.

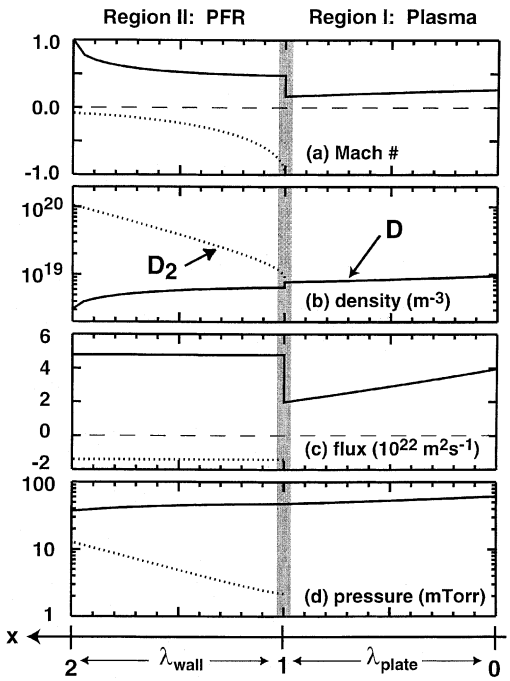

Fig. 7. Modeling results for the atom and molecule Mach number, density, flux density and total pressure (static + dynamic), bypass closed. The spatial scale for the plasma region (Region I) is $\lambda_{plate} = 5$ mm and in the private flux region (Region II) is $\lambda_{wall} = 10$ cm. Solid lines – atoms, dotted lines – molecules.

In Region I, the atom Mach number, density, flux density and pressure all decrease on moving from the target plate to the separatrix (dissociation front). Although atom pressure is conserved at the separatrix, the atom Mach number, density and flux abruptly jump – the Mach number and flux density increase to accommodate the dissociation of incoming molecules. This of course is an approximation necessitated by the analytic approach taken in this analysis. On entering Region II, the atom Mach number accelerates, reaching the sound speed at the wall, since the wall is assumed to be perfectly absorbing for atoms. The atom density drops by a factor of ~2 across Region II due to this acceleration, with a constant atom flux density.

The atom pressure drop across Region II due to interaction with the molecules, is very small in terms of a fractional change, but is important for the molecules, which are at a much lower pressure, Fig. 7(d). The momentum given up by the atoms greatly enhances the molecular pressure at the wall compared with the value at the separatrix. Thus, while the atoms are essentially collisionless with the molecules, collisional effects are important for the molecules, resulting in a molecular pressure (in this case) a factor of ~3 higher than in the absence of an atom-molecule interaction.

As expected, the molecular Mach number (Fig. 7(a)) accelerates from near stationary at the wall to sonic at the dissociation front, the molecular density decreases and the molecular flux density is constant.

4.5. Conductance limited flow

Fig. 8 gives results for the leakage fraction ϕ_1/ϕ_0 and various (static) pressures from the model applied to the C-Mod conditions described above as functions of the divertor pump fraction f. Also indicated in the figure are the corresponding values of f for bypass closed and open cases.

Two distinct regimes of operation are indicated by these results. Under highly baffled conditions, $f < 0.03$, the leakage flux is small and is linearly proportional to f, the pressures of atoms and molecules are independent of f, i.e. are determined simply by the balance between atoms leaving the plasma fan, molecules re-entering and ionization. The fraction of recycling particles pumped is

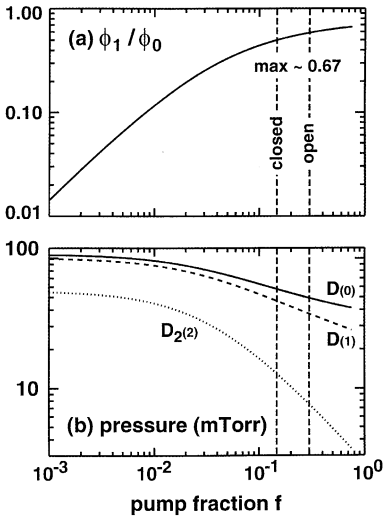

Fig. 8. Modeling results for (a) the normalized leakage flux ϕ_1/ϕ_0 (ratio of flux pumped to atom source at the target plate); (b) the atom pressure at the target plate $D_{(0)}$ and separatrix $D_{(1)}$ and the molecule static pressure at the wall $D_{2(2)}$. The results are given as a function of the pump fraction f, which is proportional to leakage conductance. The limiting value of ϕ_1/ϕ_0 according to Eq. (11) is given in the figure.

small and therefore plays little role in determining the conditions. This situation, we call 'conductance-limited' flow. This is the scenario usually envisioned for a tightly baffled divertor with opaque divertor plasma [20,21], but as one can see by Fig. 8, it is far from the present situation in Alcator C-Mod.

4.6. Flux limited flow

At higher values of pump fraction, $f > 0.03$, the leakage flux becomes nearly independent of f and the atom and molecule pressures become dependent. The effect is felt primarily on the molecular pressure outside the fan, which decreases as $\sim 1/f$, as observed on C-Mod. The atom pressures (and densities), on the other hand, are only weakly influenced, also as observed in experiment (i.e. the D_α emission shows little difference between bypass open versus closed).

This 'saturation' in leakage flux is due to a flux limit, determined by the rate of creation of atoms at the target plate and their efficiency of 'escape' out of the divertor plasma into the private flux region. This limiting leakage flux is regulated by the atomic physics (ionization and charge exchange/elastic scattering) and can be quantified by the limiting Mach number, M^* (Eq. (7)). Detailed inspection of Eqs. (5)–(7) reveals that the atom Mach number in Region I cannot exceed M^* at any point in the plasma. M^* is a function of the relative rates of ionization and momentum loss collisions and therefore, according to our assumptions, only a function of the temperature of the plasma, Fig. 9. At high plasma temperature ($T > 20$ eV), where momentum loss collisions are of less importance, M^* approaches unity, which would be expected for free-streaming atoms (fewer momentum-loss collisions). At low plasma temperature ($T < 5$ eV), where the rate of momentum loss collisions becomes greater than the ionization rate, then the limiting Mach number M^* is reduced significantly.

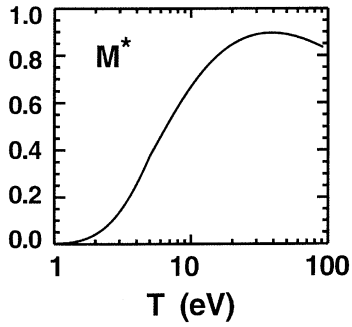

Fig. 9. The limiting atom Mach number M^* in the plasma as a function of plasma/atom temperature T.

The limiting Mach number manifests itself with respect to the escaping atom flux density limit as

$$\frac{\phi_1}{\phi_0} = \exp\left(-\frac{\lambda_{\text{plate}} M^*}{\lambda_{\text{i}}}\right). \tag{11}$$

One might note that the model results given in Fig. 8 stop at this flux limit ($\phi_1/\phi_0 \approx 0.67$), with a corresponding value of the divertor pump fraction f. At still higher values of f, the leakage flux ϕ_1/ϕ_0 would not change substantially, nor would conditions in the plasma fan, irrespective of changes in the private flux region (the molecular pressure outside the plasma would continue to decrease). Essentially, M^* is determined only by the continuity and momentum balance for atoms in the plasma, Region I (Eqs. (1)–(7)).

5. Discussion/conclusion

The primary result of this work is an understanding of the relationship between divertor leakage conductance and divertor leakage flux. In contrast to what is usually assumed, i.e. where changes in the conductance between the divertor plenum and main chamber give rise to corresponding changes in the leakage flux, our results, both experimental and through simple modeling indicate that Alcator C-Mod operates in a regime where leakage flux is nearly fixed, independent of the conductance. This is explained by operating close to a 'flux limit', where the flux is determined by the rate of neutral cre-

ation at the target plates and an escape probability out of the plasma fan and into the private flux region.

It is surprising given the relative closedness of the C-Mod divertor ($f \approx 0.15$, with bypass closed) that operation is near the limiting flux (i.e. with $\phi_1/\phi_0 \sim 1$). For example, according to our modeling, operating with a completely open divertor ($f = 1.0$) would only increase the leakage flux slightly (although a large effect on the divertor pressure would be predicted). This has to do with the compression effect of the divertor, particularly the atom-molecule interaction, which results in molecular densities very much greater than atom densities, Fig. 7(b). This allows relatively large leakage rates of molecules to the main chamber, even with a seemingly low value of the pumping fraction, $f \approx 0.15$. Clearly, to obtain low leakage rates ($\phi_1/\phi_0 < 0.1$), according to Fig. 8, the pump fraction f must be very low, $f < 0.01$, much lower than simple intuition would suggest.

The experimental results reported here have much in common with recent results from other tokamaks, including JET [3–5], ASDEX-Upgrade [6–8], DIII-D [9] and JT-60U [10]. In all cases, increasing the degree of divertor closedness increased the divertor pressure. This simple observation, by itself, effectively demonstrates that operation of these devices, as in C-Mod, had not been in the conductance-limited flow regime.

The importance of energetic atoms leaving the plasma fan and colliding with molecules outside of the plasma has never been clear in the field, e.g. [21], although an early study in the DITE bundle divertor by Fielding et al pointed out their importance in maintaining high divertor gas pressures [22]. In that experiment, gas pressures comparable to the C-Mod divertor were obtained (~30 mTorr).

In several respects, operation in the flux-limited regime is not desirable for a tokamak reactor. First, the divertor pressure is reduced from what would be possible with tighter baffling, therefore requiring higher pumping rates for fuel and gaseous impurity control. Second, the large fraction of ions striking the target plates which consequently recycle as neutrals in the main chamber may have adverse effects on confinement (although this has never been clearly shown). These results, along with results from other tokamaks, suggest that baffling needs to be significantly tighter than had been previously thought to ensure low levels of divertor leakage and maximum divertor pressures.

Acknowledgements

This work was supported by US Department of Energy Contract #DE-FC02-99ER54512. We are thankful for helpful discussions with Prof. P.C. Stangeby and Dr. N. Asakura.

References

[1] S.M. Kaye, M.G. Bell, K. Bol et al., J. Nucl. Mater. 121 (1984) 115.
[2] F. Wagner et al., in: Proceedings of the 13th International Conference, Vol. 1, Washington, DC, 1990, IAEA, Vienna, 1991, p. 277.
[3] G.C. Vlases, L.D. Horton, G.F. Matthews et al., J. Nucl. Mater. 266–269 (1999) 160.
[4] L.D. Horton, G.C. Vlases, P. Andrew, Nucl. Fus. 39 (1999) 1.
[5] R.D. Monk, JET Team, Nucl. Fus. 39 (1999) 1751.
[6] H.-S. Bosch, J.C. Fuchs, J. Gafert et al., Plas. Phys. Control Fus. 41 (1999) A401.
[7] H.-S. Bosch, W. Ullrich, A. Bard et al., J. Nucl. Mater. 266–269 (1999) 462.
[8] R. Schneider, H.-S. Bosch, J. Neuhauser et al., J. Nucl. Mater. 241–243 (1997) 701.
[9] S.L. Allen, M.E. Fenstermacher, C.M. Greenfield et al., J. Nucl. Mater. 266-269 (1999) 168.
[10] N. Asakura, N. Hosogane, K. Itami et al., J. Nucl. Mater. 266–269 (1999) 182.
[11] I.H. Hutchinson, R. Boivin, F. Bombarda et al., Phys. Plas. 1 (1994) 1511.
[12] B. LaBombard et al., presented at 14th Int. Conf. on Plasma–Surface Interactions in Controlled Fusion Devices, Rosenheim, Germany, May 2000.
[13] C.S. Pitcher, B. LaBombard, R. Danforth et al., Rev. Sci. Instrum., accepted.
[14] J.A. Goetz, B. Lipschultz, C.S. Pitcher et al., J. Nucl. Mater. 266–269 (1999) 354.
[15] C.S. Pitcher, C.J. Boswell, J.A. Goetz et al., Phys. Plasmas 7 (2000) 1894.
[16] J.A. Goetz, C.S. Pitcher et al., Submitted to Nucl. Fus.
[17] M.V. Umansky et al., Phys. Plasmas 5 (1998) 3373.
[18] P.C. Stangeby, Nucl. Fus. 30 (1990) 1153.
[19] I.H. Hutchinson, Phys. Rev. A 37 (1988) 4358.
[20] C.S. Pitcher, P.C. Stangeby, Plas. Phys. Control Fus. 39 (1997) 779.
[21] P.C. Stangeby, The Plasma Boundary of Magnetic Fusion Devices, Institute of Physics, Bristol, 2000.
[22] S.J. Fielding, P.C. Johnson, D. Guilhem, J. Nucl. Mater. 128&129 (1984) 390.